The Fields of View and Directional Response Functions of Two Field Spectroradiometers

Alasdair Mac Arthur, Christopher J. MacLellan, and Tim Malthus

***Abstract*—Accurately determining field-of-view has rarely been considered in field spectroscopy where specifications for fore optics used are generally limited and the influence of the spectroradiometer rarely considered. The issue can be compounded with full wavelength spectroradiometric systems which include multiple spectrometers. In these systems, the size and alignment of the viewing optics and technology adopted to transfer light from the fore optic to individual spectrometers may cause significant nonuniformity of spectral response across the area of measurement support, and this area may not align with that assumed from the specification that is supplied for the fore optic. When recording spectra from heterogeneous earth surface targets, it is important to have the area of measurement support accurately defined as individual reflecting surfaces may be present in varying proportions within this area, and these proportions need to be determined to relate spectral reflectance or spectral radiance to state variables or target classifications being considered. The area of measurement support and the spatial and spectral responsivity of an ASD Field Spec Pro FR spectroradiometer and a SVC GER 3700 spectroradiometer have been determined by measuring the directional response function (DRF) of each instrument. This research highlights several areas of concern and makes recommendations for the improvement of field spectroradiometers and field spectroscopy methodologies. These results are specific to the spectroradiometer/fore optic combinations investigated and at the measurement distances specified. Although similar characteristics can be expected for other instruments/fore optics of the same design, and at other measurement distances, the DRFs will vary from those reported here.**

***Index Terms*—Directional response, field of view, field spectroscopy, hyperspectral sensors, optical remote sensing, spectroradiometer.**

I. Introduction

FIELD spectroscopy is a fundamentally physically based scientific method for the quantitative measurement of spectral reflectance, radiance or irradiance in the field [1]. More specifically, it is used by a diverse group of researchers to gain an understanding of near-ground high spectral resolution reflectance, or radiance, of earth surface targets [2]–[9] and underwater surfaces [10], [11]; for the vicarious calibration of airborne and satellite data [12]–[14]; for the validation of quantitative data derived from airborne platform, or earth observing satellite, imaging sensors [15]–[17]; and for the correction of airborne or satellite acquired images for atmospheric effects [18]–[21]. The basic instrument used in this subdiscipline of hyperspectral remote sensing is the spectroradiometer, a field portable instrument capable of high spectral resolution measurements of spectral reflectance, or spectral radiance, normally at a higher spatial resolution than imaging spectrometry would acquire, and from a single sampling unit [22]. The use of spectroradiometers to capture data, typically across the 400 nm to 1000 nm or 400 nm to 2500-nm regions of the solar spectrum in approximately 200 to 500 or more contiguous bands, offers a nondestructive method to characterize target surfaces where diagnostic absorption and reflectance features or indices derived from selected wavelength regions of acquired spectra, may be related to physical and/or chemical state variables of the reflecting surfaces [23]. In addition, acquired spectra may be indicative of classifications assigned to target surfaces and related to the proportions of individual reflecting surfaces or subclasses within the area of measurement support.

To accurately estimate the reflectance of a target area in the field requires the near simultaneous measurement of two parameters: the reflected radiance from the target and the irradiance incident upon the target. The radiance reflected from the target area is normally acquired through a fixed angle fore optic, which may contain a focusing element, or through a fiber optic bundle. The irradiance incident upon the target area is normally acquired by measurement of a diffuse white reflectance reference panel by a spectroradiometer with the same fore optic arrangement as used for target measurement or by measurement using a spectroradiometer with an upward-looking cosine correcting receptor [14]. Either of these measurement configurations, termed biconical and cosconical, respectively, require target radiance and target irradiance to be ratioed to give an estimate of reflectance of the target area in the direction from which it is being measured. Only fore optics for measuring radiance will be considered here; cosine correcting receptors for measuring irradiance will not be considered further.

The area of the earth's surface from which radiance is recorded is normally considered to be delimited by the field-of-view (FOV) of the spectroradiometer's fore optic, analogous to the point spread function of satellite sensors [24], [25]. The FOV is normally defined as a solid included angle through which light incident on the fore optic or fiber optic bundle enters the spectroradiometer, and the FOV is considered by field spectroscopists to delineate the target area from which the reflected radiance is received, referred to as the area of measurement

Manuscript received May 2, 2011; revised October 2, 2011; accepted November 20, 2011.

A. Mac Arthur and C. J. MacLellan are with the Natural Environment Research Council, Field Spectroscopy Facility, School of Geosciences, University of Edinburgh, PA10 2AR Edinburgh, U.K. (e-mail: alasdair.macarthur@ed.ac.uk; chris.maclellan@ed.ac.uk).

T. Malthus is with the Environmental Earth Observation, CSIRO Land and Water, Canberra, ACT 2601, Australia (e-mail: tim.malthus@csiro.au).

Digital Object Identifier 10.1109/TGRS.2012.2185055

support [25]. The FOV is constrained by either a fore optic lens, a fore optic field stop, or the numerical aperture of the fibers in a fiber optic bundle and the optical configuration of the spectroradiometer [26], [27]. The operator can vary the size of the area of measurement support by increasing or decreasing the distance of the spectroradiometer fore optic from the target surface or by changing the fore optic. They can also vary the orientation in space of the spectroradiometer and fore optic thereby determining the angle from which the target surface is viewed.

The manufacturers of the most commonly used spectroradiometers for field spectroscopy typically only specify a nominal solid included angular value as the FOV of the fore optics supplied with their instruments (see [28] or [29], for example). However, the methods used to determine this FOV parameter are not specified, and associated uncertainties are not made explicit. Hence, the area of measurement support cannot be calculated with any degree of certainty. To determine this area accurately, the fore optic focal point needs to be known to allow height above the area of measurement support to be determined and this height, along with the included angle of the fore optic, used to calculate the radius of the FOV and hence determine the area of measurement support. For example, if a spectroradiometer with a 10° FOV fore optic was positioned such that the front of the fore optic was 0.5 m above a target surface, then the area of measurement support would vary by 12%, depending on whether the fore optic focal length was 2 cm or 5 cm, that is the focal point was 52 cm or 55 cm above the target surface. Analytical spectral devices (ASD) do suggest a method calculate the area of measurement support but appear to indicate using the front of the fore optic as the datum rather than the focal point [30] whereas spectra vista corporation (SVC), although they indicate diagrammatically that the front of the fore optic is not this datum [29], do not specify its location. In addition, the specified nominal FOV gives no indication as to the responsivity of the spectroradiometer/fore optic system to light from different positions within the area from which radiance is being measured. With no further information supplied by the manufacturers, the FOV of a spectroradiometer is assumed by users to be well defined by the included angle stated and to describe a circular area of measurement support, in the case of an ASD FieldSpec Pro, or an approximately rectangular area, in the case of a SVC GER 3700, for example. An assumption that the system has a uniform responsivity to light from different spatial locations within the area of measurement support is also often made. However, [31] indicates that when an ASD FieldSpec is used to measure the reflectance, the "anisotropic distribution of the wavelength-dependent fibers ... different areas of the surface are observed with different parts of the spectrum" resulting in steps in spectra at the joins between each detector. Therefore, this assumption of uniformity of response is erroneous, at least for this ASD instrument apparently.

To relate field radiance measurements to state variables or classes of the target being measured, or to simulations of reflectance made using optical models, there is usually a need to know precisely the area of the earth's surface from which reflected radiance is being measured. The size of this area is the sampling spatial resolution, and this resolution defines the limit of spatial detail that can be recorded by a sensor system [25]. Hence, knowledge of the sampling spatial resolution is critical particularly for heterogeneous targets, such as vegetation canopies, which consist of a 3-D structure of overlapping elements. These targets may be comprised of a number of floristic species each of which may contain spectrally distinct reflecting surfaces, and these surfaces may be present in varying proportions and with varying spatial distributions. Failure to determine the actual area of measurement support and sampling resolution and to fully characterize the system's spatial and spectral responsivity within this area, termed the directional response function (DRF) [32], may lead to uncertainties in attributing spectral reflectance or radiance to state variables or classifications of the target being measured.

Few researchers have acknowledged that it is necessary to characterize the FOV of a spectroradiometer. However, [33] using a SVC GER 1500 (which contains a single optical slit/diffraction grating/detector array spectrometer, has a spectral range of 350 nm to 1000 nm and was fitted with a "standard" fore optic) conducted an experiment to define the extent of that instrument/fore optic system's FOV. In addition, [27] measured the extent of the FOV of a SVC GER 3700 spectroradiometer instrument/fore optic system (which contains three spectrometers, has a spectral range of 350 nm to 2500 nm, and which was also fitted with a "standard" fore optic). In both of these cases, only the extent of the FOV along the instrument's principal axes was determined, and both found that the FOV generally approximated to the manufacturer's specification. However, the FOV of spectroradiometers may have greater variability than determined by [33] and [27]. In the case of the full wavelength (350 nm to 2500 nm) spectroradiometric systems investigated by [27], the multiple spectrometers incorporated may each have an influence on the area from which radiance is recorded and on the DRF as the optical path from the spectroradiometer's entrance slit to each spectrometer is unique. Measurements that could determine if the area of measurement support varied for each spectrometer were not made by [27]. In addition, neither [33] nor [27] investigated the DRF of their respective instrument. In complex spectroradiometric systems, the type, size, and alignment of the viewing fore optic and optical path from fore optic to spectrometer may cause significant nonuniformity of responsivity and wavelength dependencies across the area of measurement support.

Three criteria are proposed by [34] and [35] that can be used to assess quality of field spectroscopy measurements; traceability; repeatability; and reproducibility; and they go on to discuss the calibration chain, the need for radiometric stability, and the uncertainties introduced through variations in the illumination environment. However, field spectroscopy records spectral reflectance or radiance from an area of the earth's surface which is spatially limited by the fore optic and characteristics of the optical path through the spectroradiometer. These also affect the traceability, repeatability, and reproducibility of field spectroscopic measurements although [34] and [35] did not address them.

This paper investigates how different fore optics and optical path designs affect the area of measurement support and the DRF of spectroradiometers, to gain an understanding of the

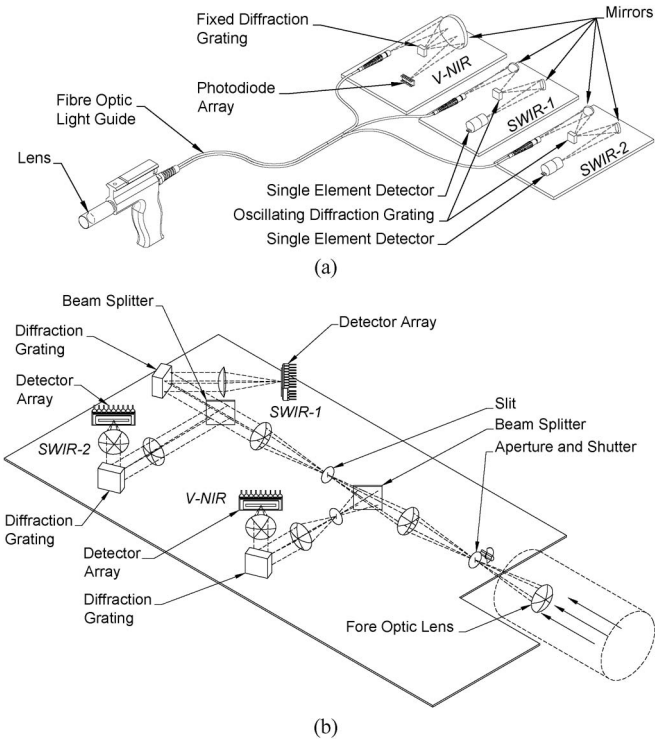

Fig. 1. Spectroradiometer optical path schematics (a) ASD FieldSpec Pro and (b) GER 3700.

spatial and spectral dependence influencing spectra recorded by these field instruments.

II. Methods

A. Spectroradiometers

The U.K. Natural Environment Research Council Field Spectroscopy Facility (NERC FSF) holds a range of portable field spectroradiometers. These instruments are made available through a peer review application process to U.K. academics for scientific research. The spectroradiometers available include ASD FieldSpec Pro FR #6449 and SVC GER 3700 #1008, and these instruments were used in this research. Both of these instruments are full wavelength systems measuring across the 350-nm to 2500-nm spectral region.

The FieldSpec Pro and GER 3700 systems use different technologies and optical designs to collect, transport, and distribute light to the three spectrometers and, in the 1000-nm to 2500-nm spectral region, also different detector technologies. The ASD FieldSpec Pro uses a fore optic, either a fixed focus lens or a field stop with no focusing lens element, to collect radiance and distributed it via a fiber optic bundle to a fixed diffraction grating spectrometer for the 350-nm to 1000-nm, visible near infrared (VNIR), spectral region, and two oscillating defraction grating monochromators with cooled single element indium gallium arsenide detectors for the 1000-nm to 1750-nm, first short wave infrared (SWIR-1), and 1750-nm to 2500-nm, second SWIR-2, spectral regions [Fig. 1(a)]. The fiber optic bundle contains 57 individual fibers (of 110 μm and 220 μm diameter for the VNIR and SWIR fibers, respectively), and the position of each fiber within the bundle is determined

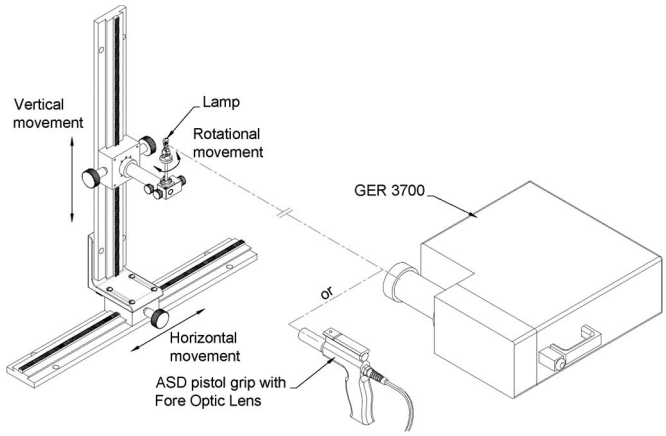

Fig. 2. Measurement configuration showing direction of movement of linear stages, rotation of lamp, and position of ASD FieldSpec Pro or GER 3700.

through a random process at time of the bundle manufacture with 19 fiber subsequently being distributed to each of the three spectrometers [30]. Therefore, the ASD FieldSpec Pro optical fiber distribution may be unique to each instrument. The GER 3700 is typically configured with a fixed focus fore optic lens (although a fiber optic accessory is available) attached to the spectroradiometer with radiance received distributed using lenses, mirrors, beam splitters, and optical slits to a fixed diffraction grating/photodiode array spectrometer covering the VNIR spectral region and two fixed diffraction grating/lead sulphide array detector assemblies for the SWIR-1 and SWIR-2 spectral regions [Fig. 1(b)].

B. Measurements

All measurements to characterize the DRF and FOV of the two spectroradiometer systems were carried out in an optical darkroom custom built for spectroradiometric system calibration and measurements at the NERC FSF. A 55-cm linear stage, with micrometer adjustment, was mounted on an optical table within the darkroom and a second 55-cm linear stage, also with micrometer adjustment, mounted orthogonally on the movable carriage of the first stage. A miniature 20-W quartz tungsten halogen lamp, with a 4 mm $\times$ 0.7 mm coiled filament, was then mounted on a rotary stage (also with micrometer adjustment) and secured, in the horizontal plane, to the movable carriage of the vertical linear stage (Fig. 2). This configuration allowed the lamp to be moved vertically and horizontally across the area defined by the nominal FOV of each instrument and the lamp to be rotated horizontally. A miniature laser diode was mounted on the vertical center line of the rotary stage and, when the stage was rotated horizontally, was used to ensure that the same point of the lamp filament was aligned with the geometric center line of each fore optic for each measurement. A quartz tungsten halogen lamp was selected as it emits a high intensity, continuous light across the spectral range of interest in this research. A regulated stabilized power supply was used to ensure lamp output stability for the duration of the measurements. The darkroom walls were black and spectrally flat with a reflectance of less than 5% and black spectrally flat optical cloth, also with a reflectance of less than 5%, covered the optical table and the

vertical linear stage to reduce spurious reflections from the light source. The lamp was centered on both linear stages and on the rotary stage and this position used as the reference point (the "zero" point) for all subsequent measurements. The working distance between the lamp and the front of the fore optics was set at 1 m and kept constant for all reference measurements, except for measurements made using the GER 3700 fiber optic bundle where a distance of 500 mm was used. This reduced working distance was used for the GER 3700 with fiber optic bundle due to concerns that spurious reflectances could be integrated into the measurements when the light was positioned toward the responsivity limits closest to the optical bench as the fiber bundle could have had a FOV of approximately 25°.

The geometric center line of each spectroradiometer's fore optic was aligned with the center line of the lamp, and for the ASD, the optimization routine was first initiated, then a reference spectral measurement of the lamp acquired. The reference measurement was followed by acquiring a target measurement spectrum of the lamp without moving any of the stages. The lamp was then moved in 5-mm increments, both horizontally and vertically, for both the ASD FieldSpec Pro with 10° fore optic and the 5° fore optic measurement sequences and a target spectrum acquired at each point to complete a grid of measurement points. For the FieldSpec Pro/bare fiber bundle system measurements, a more sparse sampling strategy was adopted as can be seen in Fig. 7. For the GER 3700 10° fore optic measurement sequence, the lamp was moved in 1-cm increments, both horizontally and vertically, and target spectra acquired as for the ASD system. For the GER system with the 3° fore optic and with the fiber optic accessory, only the principal axes of the area defined by the nominal FOV were sampled in 1-cm increments. The spatial extent of the measurement sequences were determined by continuing to take measurements until the maximum height of any point of the spectrum measured was less than 2% of the reference measurement spectrum, when it became difficult to visually differentiate the spectra on the control computer screen. After each horizontal and vertical sequence of measurements, the lamp was returned to the reference point, and another reference measurement taken. In total, some 7250 spectra were acquired for analysis.

C. Postprocessing and Data Analysis Methods

Processing of the ASD data required a normalization adjustment to each spectral data file to account for the VNIR channel integration time and SWIR-1 and SWIR-2 gain settings determined by the instrument during the optimization routine. The data from each spectroradiometer/fore optic configuration and for each wavelength selected for analysis were then normalized to the maximum amplitude measured for that wavelength within the measurement field. To enable the spectra to be spatially located, the positional coordinates of each measurement point recorded from the linear stage micrometers were appended to the spectra data files recorded by each spectroradiometers. After initial analysis, the data files were reduced to a selected number of wavebands typifying the reponsivity of each spectrometer of each instrument/fore optic, for final analysis and display.

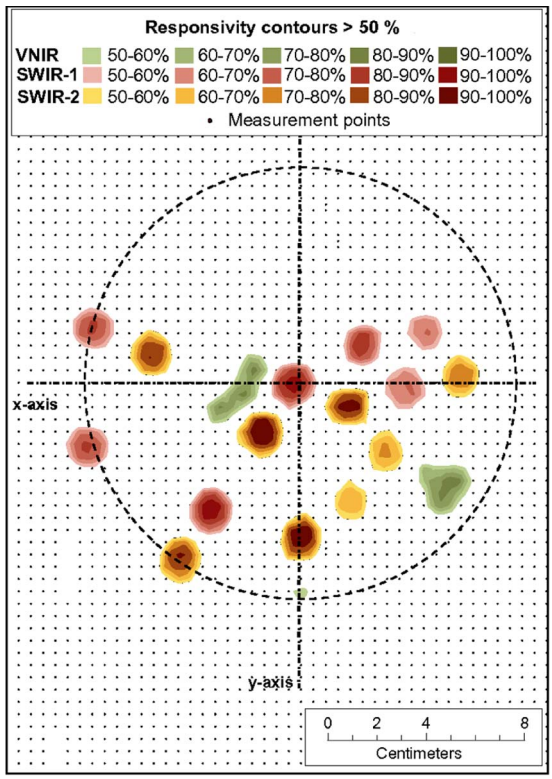

Fig. 3. ASD FieldSpec Pro DRF greater than 50% response with the nominal 10° fore optic.

As consideration is being given here to the spatial distribution of responsivity of spectroradiometric systems that measure from a continuous field only varying in levels of spectral intensity and at contiguous wavelengths, the points of measurement are considered to be spatially autocorrelated. Therefore, a geostatistical approach was adopted to analyze and display the data and, for each wavelength selected for display, an ordinary kriging routine was used for spatial interpolation. Ordinary kriging provides a 2-D probability interpolation method using a weighted linear combination of available data with the aim of minimizing errors of variance [36] and provides a unbiased estimator [37]. In addition, kriging allows for a statistical estimation of error of the responsivity across the area of measurement displayed at the specific contours levels selected, where no measurement data may have been acquired. By adopting such a geostatistical approach a 2-D graphical representations of the area of measurement support, and DRF across this area, for each instrument/fore optic combination at each selected wavelength, could be produced with contours selected for display by levels of spectroradiometric system responsivity.

III. Results and Discussion

A. ASD Fieldspec Pro Area of Measurement Support and DRF With a 10° Fore Optic Lens

The geostatistically interpolated DRFs, for this instrument/fore optic/measurement distance combination, at three wavelengths (700 nm, 1500 nm, and 2200 nm), each typifying the response of the VNIR, SWIR-1, and SWIR-2 spectrometers, respectively, of the ASD instrument are displayed in Fig. 3 where a lower limiting contour of 50% of the maximum

responsivity level has been chosen. The hatched circle in Fig. 3, with a diameter of 17.5 cm, represents the spatial extent of the nominal FOV specified by the manufacturer for this fore optic using their suggested method of calculation [30]. The position of each area of responsivity is indicative of the position of individual fibers in the fiber optic bundle and their distribution to the individual spectrometers, where the responsivity is greater than this 50% level. The response of the instrument to radiant flux can be seen to be sparse with little or no coverage of significant areas within the area defined by the nominal FOV at this level of responsivity. The responsivity is concentrated in the lower half of the nominal FOV, with the distribution spatially dependent and highly irregular. The elongated area left of center in Fig. 3 indicates that three fibers attached to the VNIR spectrometer are adjacent to each other in the bundle, as does the triangular area in the bottom right quadrant nearest to the nominal FOV limit. However, given the spatial sampling resolution selected and the diameter of the fibers in the bundle, the position of some fibers may possibly not be displayed at this 50% responsivity level.

To investigate the area of measurement support and the DRF of this ASD system at this measurement distance further, a lower limiting contour of 5% of the maximum responsivity level for the same wavelengths as previously considered was selected and the interpolated data displayed in Fig. 4. Again, each area of responsivity indicates of the position of individual fibers in the optical fiber bundle, but for each spectrometer of the ASD used in this work, only 16 fibers are evident for each spectrometer, rather than the 19 specified by ASD, suggesting that three fibers may not be transmitting light to each spectrometer. The nonshaded areas in Fig. 4(a), (b), and (c) indicate areas where the radiance received by each of the spectrometers is less than 5% of the maximum normalized response. The VNIR spectrometer responsivity at the 5% level is largely distributed to the outer regions of the nominal FOV with little coverage toward the center [Fig. 4(a)], although the concentration of coverage at the two locations where three VNIR fibers appear to be adjacent to each other is again evident. The VNIR spectrometer also has significant responsivity to areas outside the nominal 10° fore optic FOV. The SWIR-1 spectrometer displays little responsivity in the lower right quadrant, the bias being toward the other three [Fig. 4(b)] and with less responsivity to areas outside of the nominal FOV than displayed by the VNIR spectrometer. The SWIR-2 spectrometer responsivity is biased to the lower half of the nominal FOV with little in the upper two quadrants [Fig. 4(c)], and also with less responsivity evident to areas outside the nominal FOV than the VNIR spectrometer. The area of measurement support normally assumed by field spectroscopists (the nominal FOV) is generally within the 5% DRF contour, but for all three channels, the coverage within this area varies significantly. The areas of maximum responsivity are variable for all three spectrometers, and in some cases, the responsivity peaks are less than 50% of the maximum. The combined DRF data for the three spectrometers, with the lower limiting contour of 5% of the maximum responsivity level for each of the selected wavelengths displayed, highlight the strong spatial dependency of the spectroradiometer system responsivity [Fig. 4(d)]. The nonshaded areas in Fig. 4(d) indicate "blind spots" for the spectroradiometer where little or no radiance is being measured and integrated into the full wavelength (400 nm to 2500 nm) spectrum being recorded.

Cross-sectional plots of the responsivity of the system, at the selected wavelengths, along the x-axis and the y-axis of Fig. 4(d) are displayed in Fig. 5(a) and (b), respectively. These figures highlight the strong spatial and spectral dependencies and the response of the system to radiant flux from outside of the 17.5-cm diameter nominal FOV. The narrow, approximately Gaussian, response and point of maximum normalized responsivity for each fiber receiving radiant flux is also evident from these figures.

When this 10° lens-based fore optic is used, the areas of responsivity for each of this ASD's three spectrometers are individually distinguishable and their spatial distribution uneven within the nominal FOV specified by the manufacturer. Therefore, the area of measurement support and the area assumed from the nominal FOV are not the same. However, the number and location of the responsivity peaks appear to align with individual fibers in the fiber optic bundle and each area of response to the distribution of the fibers to the spectrometers. This indicates that the area of measurement support is being imaged by the 10° lens onto the tip of the fiber optic bundle such that each individual fiber is receiving radiance from different spatial locations within the area of measurement support and transmitting that to the individual spectrometers to which each fiber is aligned during manufacturing. Consequently, each spectrometer is measuring radiance from different spatial locations. The regions of the full wavelength spectrum measured by each spectrometer are thus from distinctly different areas, with responsivity being "weighted" by location. At the 5% limit of peak responsivity, which contains approximately 95% of the total reflectance, there is little overlap of the areas sampled by each spectrometer. Hence, full spectral information is acquired from few regions within the area of measurement support, and it is evident that specifying an albeit nominal FOV for the ASD FieldSpec Pro with 10° fore optic is highly misleading.

The ASD FieldSpec Pro has a number of different optical accessories available including a nominal 5° FOV fore optic, again with focusing element, and an 18° FOV field stop with no focusing element. The area of measurement support and the DRF of both of these fore optic accessories will now be considered.

B. ASD Fieldspec Pro Area of Measurement Support and DRF With a Nominal 5° Fore Optic Lens

The general design of the ASD fore optic lens accessories are the same and the DRF of the 5° nominal FOV fore optic used in this work was found to display similar characteristics to those of the system with the 10° lens [Fig. 6(a)], when sampled at the same measurement distance. Spatial coverage of the area within the nominal FOV at the 5% responsivity level was not quite complete, although coverage was proportionally more extensive than with the 10° fore optic. The responsivity of the system was again "weighted" by location. However, the responsivity at the 5% level from outside the nominal FOV for the 5° fore

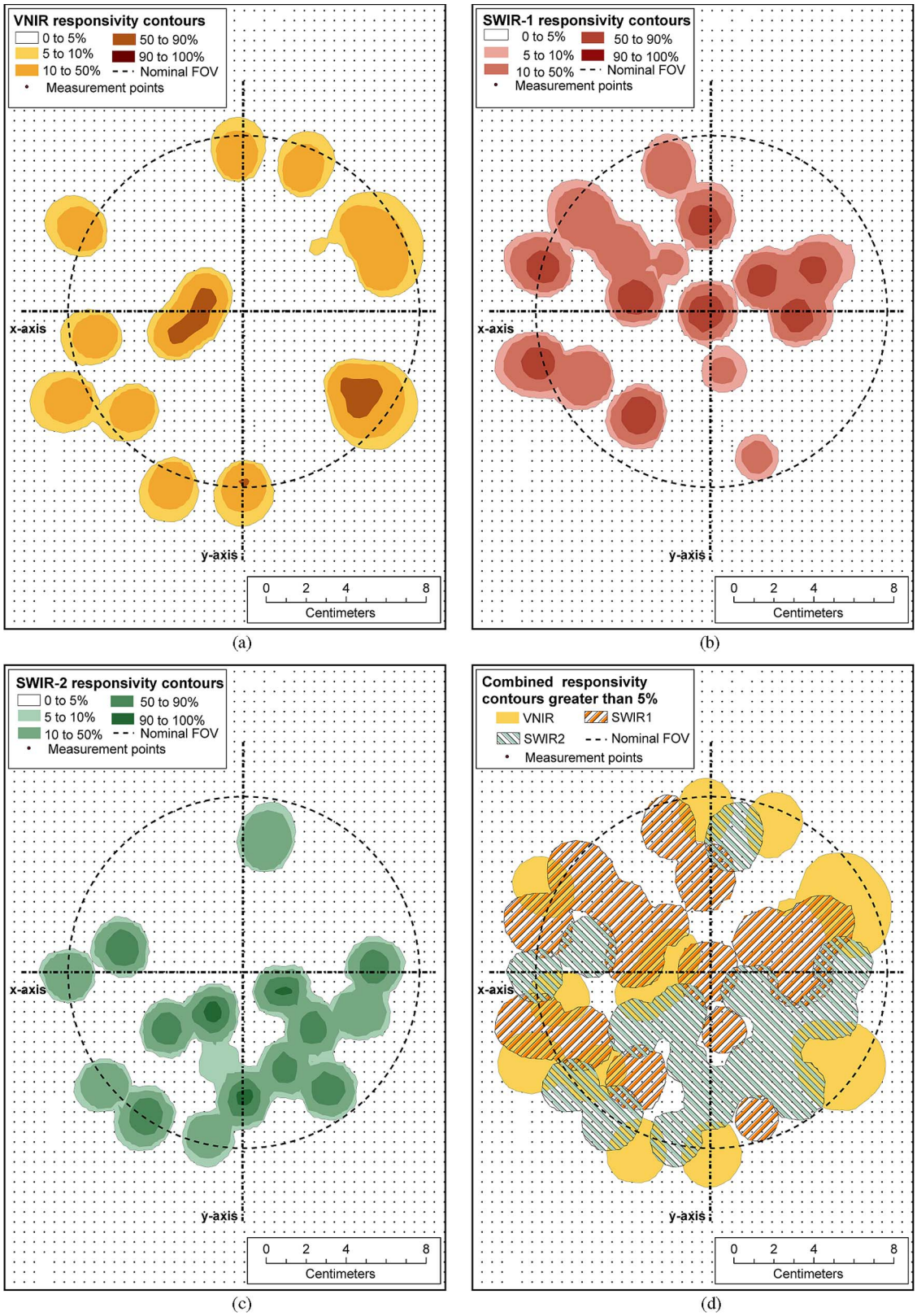

Fig. 4. ASD FieldSpec Pro DRF greater than 5% response with the nominal 10° fore optic. (a) VNIR. (b) SWIR-1. (c) SWIR-2. (d) VNIR, SWIR-1, and SWIR-2 combined.

optic was minimal. The size of the areas within the area of measurement support with a responsivity greater than 50% was found to be smaller for this optic than that for the 10° fore optic as can be seen in Fig. 6(b) from the width of each Gaussian response for each fiber recording radiance from along the line of the x-axis of Fig. 5(a).

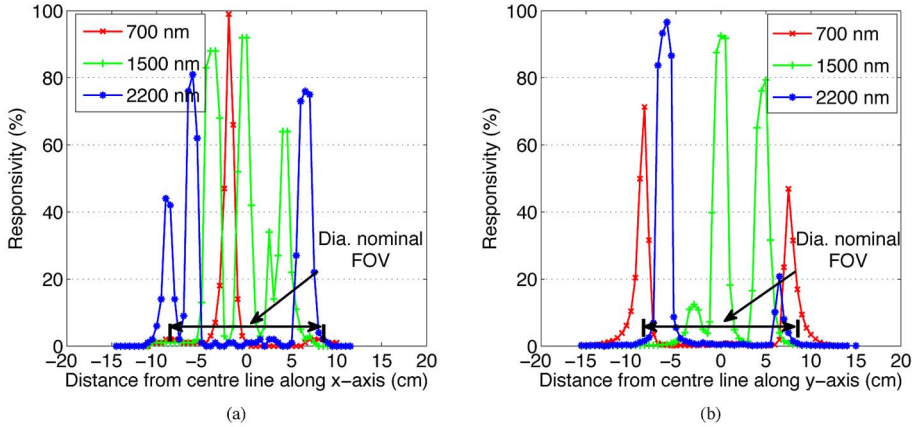

Fig. 5. DRF cross section along the major axes of the ASD FieldSpec Pro with 10° fore optic. (a) x-axis cross section. (b) y-axis cross section.

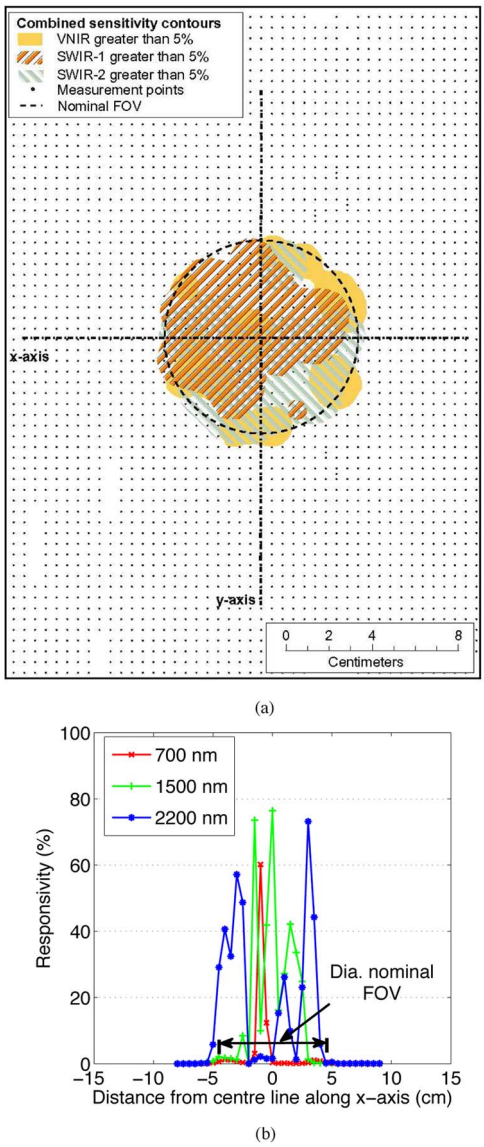

Fig. 6. DRF cross section along the x-axis of the ASD FieldSpec Pro with 5° fore optic. (a) 5% DRF contours. (b) x-axis cross section.

When this 5° lens-based fore optic is used, the areas of responsivity of each of the three spectrometers can still be differentiated, although there was significantly greater overlap between them than evident for the 10° fore optic. Radiance was received by at least one spectrometer from all areas within the nominal FOV. In addition, at both the 5% and 50% responsivity levels, the total extent of the area of measurement support approximates more closely to that which could have been assumed from the manufacturer's specification for this lens-based fore optic than for the 10° fore optic.

C. ASD Fieldspec Pro Area of Measurement Support and DRF With a Nominal 18° Field Stop Fore Optic

The DRF of this ASD spectroradiometer with its 18° fore optic at this measurement distance displays different characteristics to that displayed when lens-based fore optics are used. Greater spatial and spectral uniformity are evident, and the areas of responsivity of the spectrometers can be seen to be primarily concentric and evenly distributed (Fig. 7). The 18° fore optic comprises a field stop, and, as there is no focusing element present, the area of measurement support appears not to be imaged onto the tip of the fiber optic bundle. Hence, each spectrometer can be considered to have a FOV rather than each fiber, as was the case for the lens-based fore optics. For the VNIR spectrometer, the area with a 50% responsivity level approximates to the area of that would be assumed from nominal FOV, although the areas of measurement support of the SWIR-1 and SWIR-2 spectrometers are slightly less. At the 5% responsivity level, the area of measurement support also varies for each spectrometer. At this level, the area of measurement support for the VNIR spectrometer is slightly larger than the area of the nominal FOV [Fig. 7(a)]; the area of measurement support of the SWIR-1 spectrometer approximates to the nominal FOV [Fig. 7(b)]; and that of the SWIR-2 spectrometers can be seen to be significantly less than the area of the nominal FOV [Fig. 7(c)]. From Fig. 8, it is evident that at the 50% responsivity level, the area measured by the VNIR spectrometer is greater in diameter than that of the SWIR spectrometers and that the SWIR spectrometer FOVs are closely aligned. The responsivity of the spectrometers in the ASD system with this 18° fore optic has approximately a Gaussian distribution as can be seen from Fig. 8(a) and (b). From these figures, it can also be observed that for the VNIR spectrometer, the diameters of the 5% and the 50% sensitivity contours approximate to each other, although

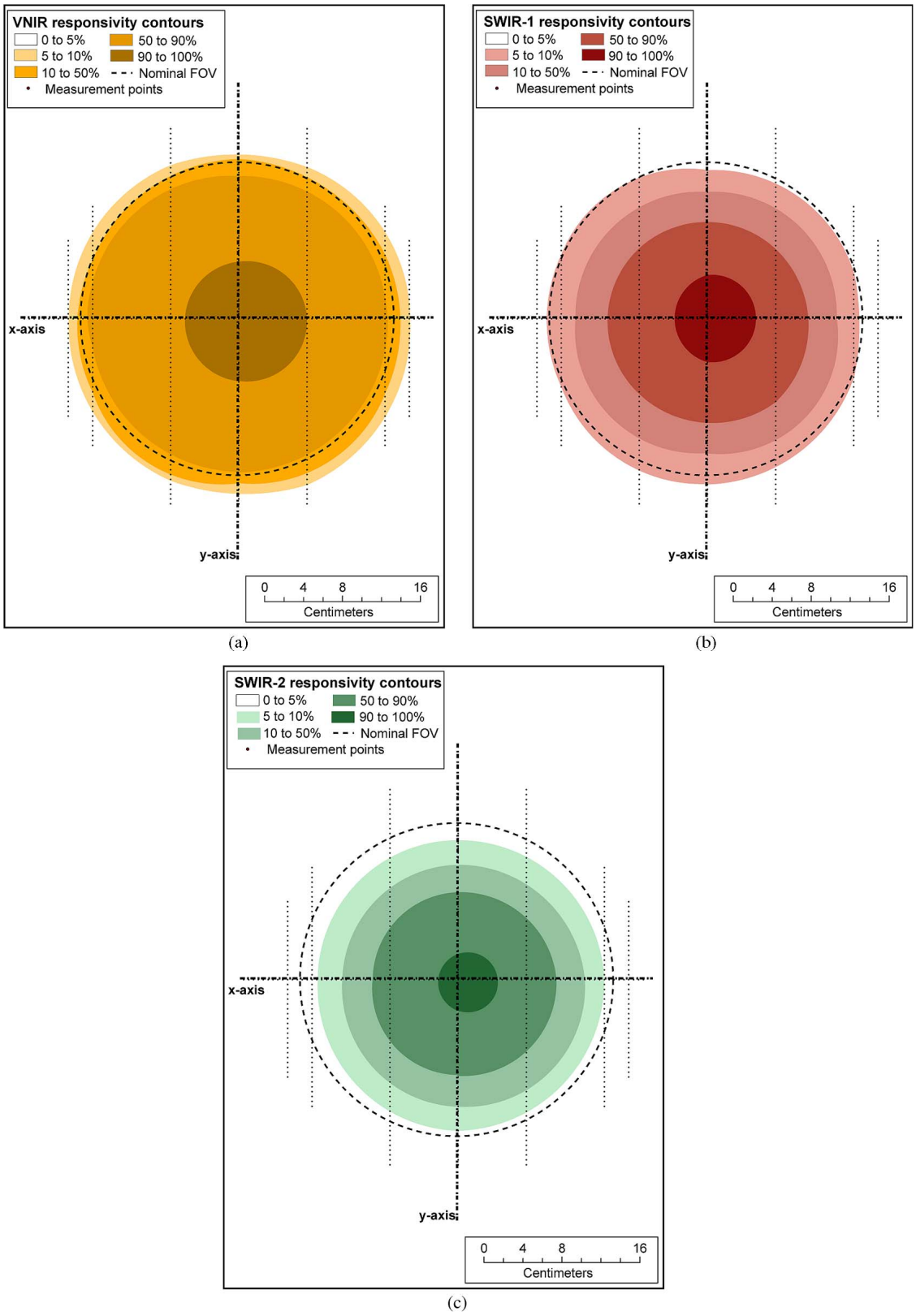

Fig. 7. ASD FieldSpec Pro DRF greater than 5% response with the nominal 18° fore optic. (a) VNIR. (b) SWIR-1. (c) SWIR-2.

there are significant differences in diameter between the 5% and the 50% responsivity contours for the SWIR spectrometers.

The difference between the VNIR and SWIR spectrometer FOVs at the 50% responsivity level, and the similarities at the 5% responsivity level, may indicate that it is the field stop that is restricting the VNIR spectrometer's FOV, while the FOV of the SWIR spectrometers is possibly being restricted by the numerical aperture of the fibers. The numerical aperture

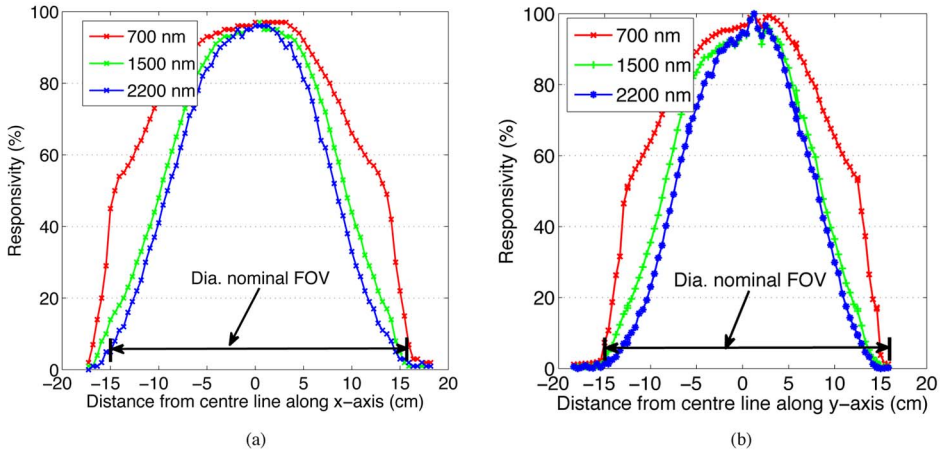

Fig. 8. DRF cross section along the major axes of the ASD FieldSpec Pro with 18° fore optic. (a) x-axis cross section. (b) y-axis cross section.

of each of the fiber diameters (110 and 220 μm) included in the fiber optic bundle are not specified by ASD, although they do advise that the FOV of the "bare" fiber bundle is 25° [30]. The apparent difference in numerical aperture between the 110 μm and 220 μm fibers may be due to the material used for the fiber of the cores, and possibly the cladding, of each of the VNIR and SWIR fibers being different. The SWIR fiber diameter and core and cladding material may have been chosen to optimize light transmission in the SWIR spectral range, while those used for the VNIR fibers chosen to suit the spectral range of that spectrometer. However, at the 5% responsivity level, the FOV of all three spectrometers are close to being in alignment. From the foregoing, it is evident that the area of measurement support and DRF of the ASD FieldSpec Pro with this 18° fore optic more closely approximates to that assumed by field spectroscopists than do the areas of measurement support and DRFs of this ASD system with these lens-based fore optics, although there are still differences.

D. GER 3700 Field Spectroradiometer Area of Measurement Support and DRF With a 10° FOV Lens

Within the GER 3700 spectroradiometer, a different technological approach has been adopted to transfer light from the fore optic to the spectrometers [Fig. 1(b)] than that used in the ASD FieldSpec Pro. Hence, the area of measurement support and the DRF of the GER 3700 display different phenomena to those of the ASD system. From Figs. 9 and 10, it can be seen that the GER 3700 is responsive to radiance from contiguous areas within the nominal FOV of each of its spectrometers, although the FOVs of each spectrometer do not necessarily align with each other or match the manufacturer's specified nominal FOV for the 10° fore optic. The VNIR spectrometer 50% responsivity contour delineates an irregular area rather than a circle, although it is completely contained within the nominal FOV of the 10° fore optic (Fig. 9). However, the extent of the VNIR 5% sensitivity contour exceeds the nominal FOV for approximately half its diameter at 700-nm [Fig. 9(b)] and 900-nm [Fig. 9(c)] wavelengths, while at the 450-nm [Fig. 9(a)] wavelength, the 5% contour is mainly within the nominal FOV. The peak responsivities for each of the wavelengths displayed in Fig. 9 are within the nominal FOV, although there is a marked shift from the left to right along the x-axis of the area of measurement support. Thus, spectral reflectance to the right side of the nominal FOV has a responsivity bias to blue wavelengths [Fig. 9(a)] compared to the left side where the spectrometer has its maximum responsivity to infrared wavelengths [Fig. 9(c)], while the greatest responsivity to red wavelengths is approximately in the middle of the nominal FOV [Fig. 9(b)]. There are areas within the nominal FOV, primarily to the left for blue wavelengths [Fig. 9(a)] and to the right for infrared wavelengths [Fig. 9(c)], from which little or no reflected radiance is integrated into the full wavelength spectrum recorded. The GER 3700 is responsive through its full wavelength range (400 nm to 2500 nm) to radiant flux from the central region of the nominal FOV. However, both SWIR spectrometers have areas of responsivity to the left and to the right of the nominal FOV from which little or no radiance is integrated into the measurement recorded, and both display an approximately rectangular area of measurement support [Fig. 10(a) and (b)]. The right to left bias of blue through red to infrared wavelengths, along the x-axis of Figs. 9 and 10, is evident in Fig. 11(a) where the location of the point of maximum responsivity for each of the wavelengths displayed can be seen. From Fig. 11(b), it is evident that the points of maximum responsivity are more close to being central on the y-axes of Figs. 9 and 10 and aligned with the optical slit of the spectroradiometer.

Unlike the ASD system, each spectrometer in the GER 3700 is responsive to radiance from a significant and overlapping central region of the area of measurement support. Nevertheless, the areas from which radiance is recorded by each of the three spectrometers in the GER 3700 with 10° fore optic are also individually distinguishable. There are areas within the nominal FOV to which one or other of the three spectrometers receive little or no radiant flux and the DRF of the VNIR spectrometer is wavelength dependent with a right-to-left/blue-to-infrared responsivity bias. The design of the fore optic; the unique optical path from the instrument's entrance slit to each of the three spectrometers; the size and location of spectrograph slits; and the magnification factors of the various elements within each optical path may all influence the extent of the areas

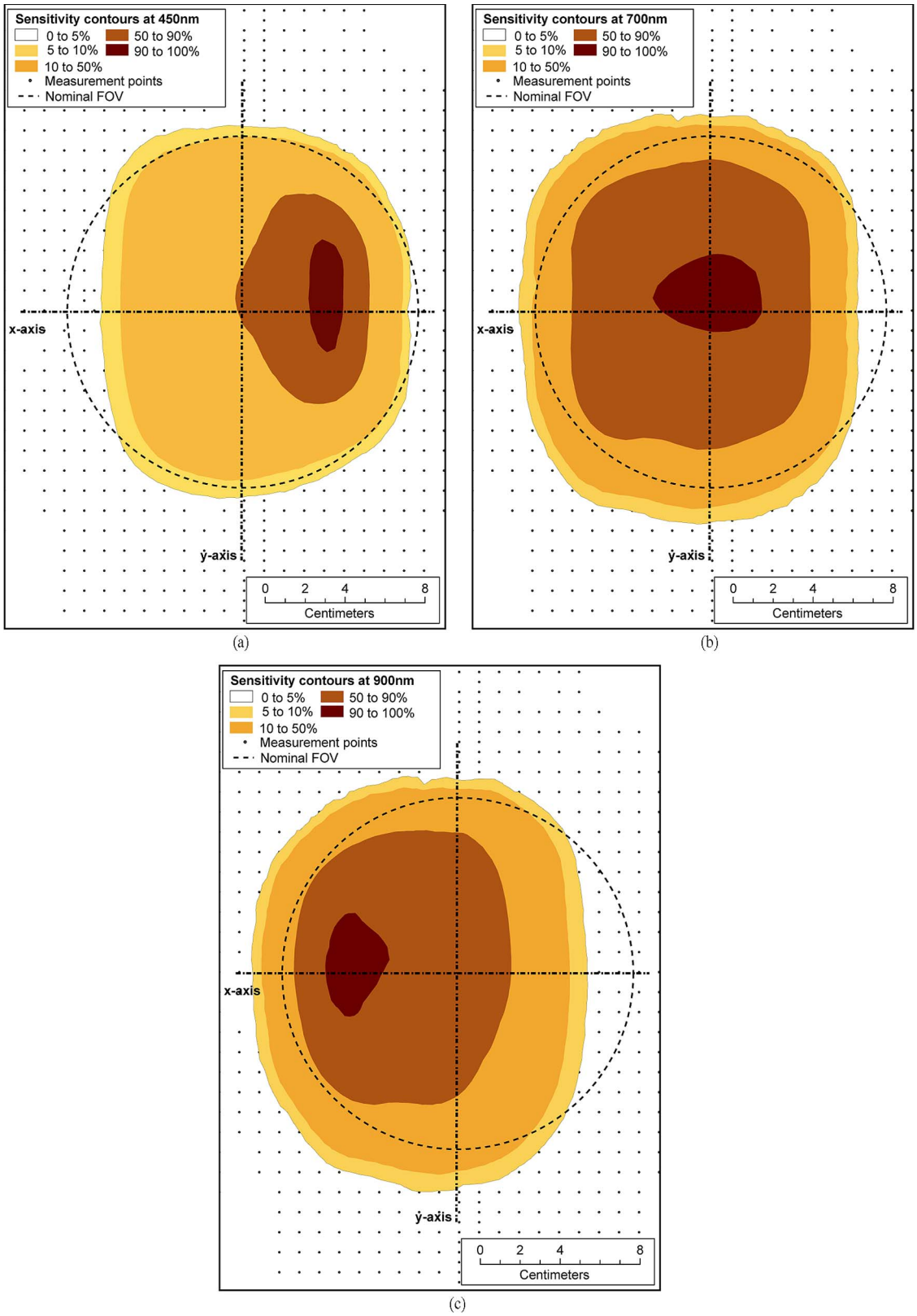

Fig. 9. GER 3700 with 10° fore optic VNIR DRFs at selected wavelengths. (a) 450 nm. (b) 700 nm. (c) 900 nm.

of measurement support and the DRF of each spectrometer and, hence, those of the combined GER 3700 spectroradiometric system.

E. GER 3700 Field Spectroradiometer Area of Measurement Support and DRF With a Nominal 3° Lens

The area of measurement support and DRF of the GER 3700 fitted with its 3° lens, the "standard" GER fore optic,

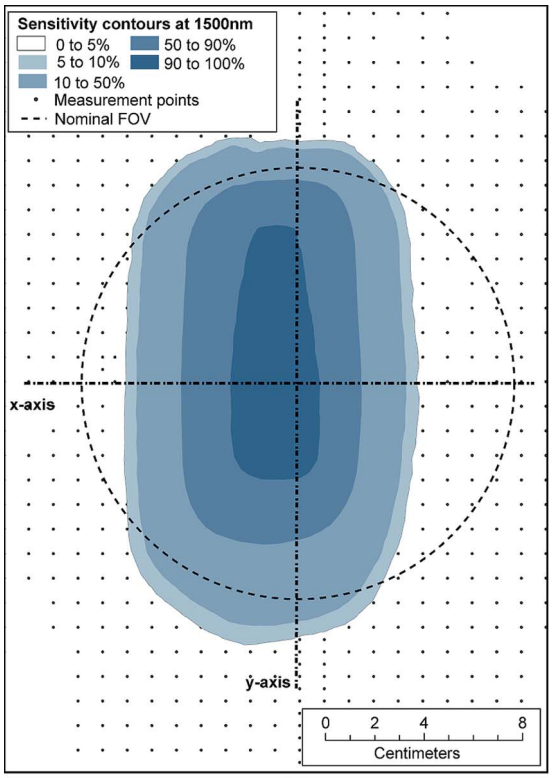

Fig. 10. GER 3700 with 10° fore optic SWIR DRFs at selected wavelengths. (a) 1500 nm. (b) 2200 nm.

was also assessed and found to display similar, although less pronounced, characteristics to those found with the 10° fore optic fitted. The VNIR right-to-left blue-to-infrared spectral responsivity shift was still evident as the blue wavelengths were

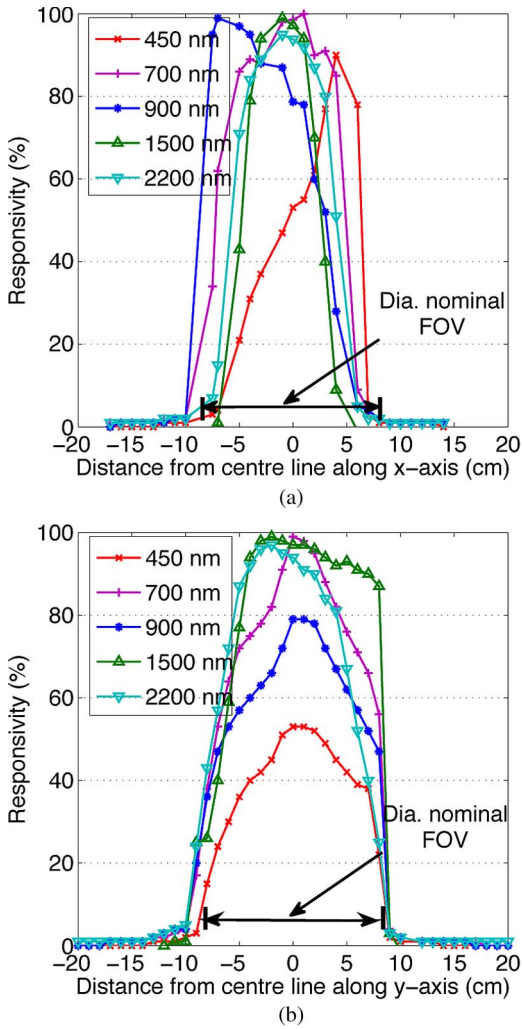

Fig. 11. DRF cross section along the major axes of the GER 3700 with 10° fore optic. (a) x-axis cross section. (b) y-axis cross section.

again found to have a maximum sensitivity toward the right of the FOV (across the optical slit) and infrared toward the left [Fig. 12(a)]. However, response to infrared wavelengths was more evenly distributed than observed with the 10° fore optic fitted. Along the line of the instrument's entrance slit, there appeared to be no spectral shift for VNIR wavelengths as the maximum responsivity of each was approximately aligned with the y-axis of the area of measurement support [Fig. 12(b)]. The 5% and 50% responsivity contours were found to be reasonably well aligned with each other along the x-axis [Fig. 12(a)], although a slight responsivity bias to the right of the x-axis was evident for the blue wavelengths. Along the y-axis, the 5% and 50% responsivity contours were less well aligned [Fig. 12(b)]. The 5% and 50% responsivity contours for each spectrometer are more closely aligned for the 3° fore optic than for the 10° fore optic, as can be seen by comparing Figs. 11 and 12. The area of measurement support is considered to again be rectangular at the 5% responsivity level as it measures approximately 8 cm along the x-axis and 10 cm along the y-axis, due to the influence of the optical slit. However, at the 50% responsivity level the area of measurement support is more square with axes of approximately 7 cm.

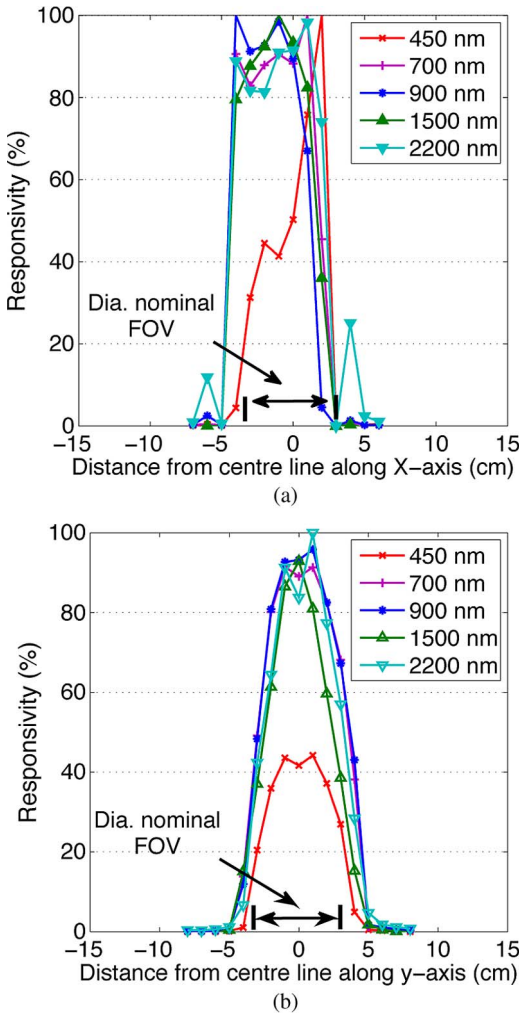

Fig. 12. DRF cross section along the major axes of the GER 3700 with 3° fore optic. (a) x-axis cross section. (b) y-axis cross section.

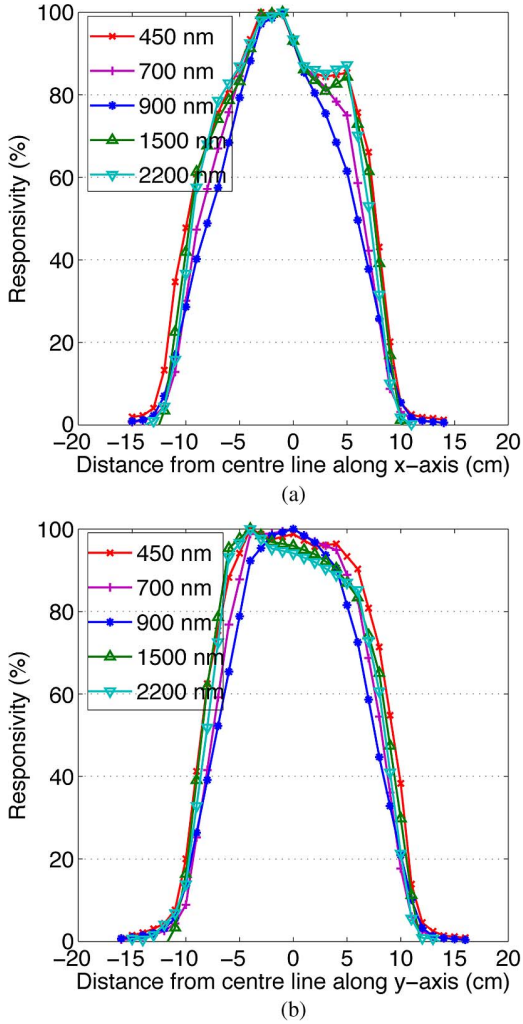

Fig. 13. DRF cross section along the major axes of the GER 3700 with fiber optic fore optic at a distance of 500 mm from target. (a) x-axis cross section. (b) y-axis cross section.

As was observed for the GER system with the 10° fore optic, the response to radiance by each spectrometer overlapped in the central region of the area of measurement support, although the areas of measurement support of each of the spectrometers remained distinguishable, particularly for the VNIR detector. There remains a blue to infrared/right to left responsivity bias, although it is less pronounced than for the 10° fore optic. However, unlike the system with the 10° fore optic, there were no areas within the nominal FOV from which radiant flux was not received by a spectrometer. It is therefore evident that the DRF and area of measurement support more closely aligns to that which would be assumed from the specification for the 3° fore optic, although it is more extensive at both the 5% and 50% responsivity levels.

F. GER 3700 Field Spectroradiometer Area of Measurement Support and DRF With a Fiber Optic Attachment

A fiber optic accessory is available for use with the GER 3700, although presently, there is no FOV limiting fore optic attachment supplied. The fiber optic bundle contains 400 individual fibers, each of the same diameter. However, the nominal FOV of this accessory has not been specified by the manufacturer. From these measurements, the area of measurement support was found to be circular, measuring approximately 18 cm along each major axis at the 50% responsivity level and approximately 24 cm along each major axis at the 5% responsivity level [Fig. 13(a) and (b)]. It can also be seen that the width of the area of measurement support at the 5% responsivity level is approximately 6 cm greater than at the 50% level. Hence, if the nominal FOV of the fiber optic accessory is calculated from this data, at the 5% responsivity level, it is approximately 27°, and at the 50% responsivity level, it is approximately 20°. Furthermore, the responsivity was found to be approximately Gaussian and concentric for each of the wavelengths displayed, although the area of maximum responsivity is wider across the y-axis [Fig. 13(b)] than the x-axis [Fig. 13(a)]. The fibers in the fiber optic bundle supplied for the GER 3700 are mixed during manufacture such that the position of each fiber at one end of the bundle is not the same as that fiber's position at the other end of the bundle and, as each fiber can be assumed to have a circular FOV the area of measurement support will be circular, with little influence from the optical slit.

The GER 3700 system with fiber optic accessory displays no spectral left to right bias and the area of measurement

support and DRF of each spectrometer align more closely with each other than was found with the other fore optics. The response to radiance by each spectrometer covers the full area of measurement support, and there were no areas within this from which radiant flux was not received by each spectrometer. In addition, and again unlike the GER optics previously assessed, when using the fiber optic accessory, the area of measurement support of each spectrometer were primarily indistinguishable.

These area of measurement support and DRF characteristic differences between the fiber optic and lens-based fore optics for the GER 3700 system indicate that, similar to the ASD system, the area of measurement support is being imaged into the optical path by the lens-based optics. As there was no responsivity bias when using the GER 3700 fiber optic accessory, which does not have a focal point, it would appear to be the dimensions and design of the lenses and where their points of focus fall within the optical path that are the cause of the spectral bias. This is also indicated by the DRF differences observed between the 10° and the 3° fore optic data, where the focal point of each will fall at different locations within the optical path. In addition, it would appear to be the shape and dimensions of slits and detector arrays that cause the area of measurement support to be elongated rather than circular for the lens-based fore optics.

G. Measurement and Responsivity Contour Uncertainties

The uncertainties associated with the extent of the areas of measurement support and DRFs displayed are dependent on both systematic and random errors introduced during measurement and from the interpolation method adopted for the analysis. Systematic errors will result from spectroradiometric uncertainties such as in wavelength position and detector response linearity and uncertainties introduced by the physical dimension of the lamp and the spatial sampling resolution adopted. As the size of the light source used limited the maximum possible spatial resolution of the measurements, the point of absolute maximum responsivity for an individual wavelength interval may therefore fall between two measurement points. This may result in only the apparent maximum being used to normalize the data, thus the DRFs displayed are relative rather than absolute measures. Random errors will result from uncertainties related to the lamp's position and rotation, relative to the fore optic geometric center line, and from spectroradiometric dark current and thermal stability errors. Errors introduced by spatial interpolation include the number, proximity and spatial arrangement of samples, the nature of the phenomena being studied (is it a continuous smooth field, for example) and the interpolation model selected. Systematic spectroradiometric errors are quantified during the routine quality assurance procedures applied to both instruments and are minimized by recalibration of spectroradiometer if required and will not be discussed further here. Uncertainties introduced through the spatial sampling resolution are quantified during the interpolation accuracy assessment.

As during the spectral measurement sequence, the reference spatial location of the lamp (the measurement axis "zero" point) was repeatedly measured, the spectral measurements at this location have been used to determine a statistical confidence level for the spectroradiometer/fore optic system responsivity which integrates both positional and spectroradiometric uncertainties. For a 95% confidence level, the measurement error at the "zero" point was calculated to be better than $\pm 5.5\%$ with 35° of freedom for the GER 3700 system with 10° fore optic and for the ASD system with the 10° fore optic. The uncertainty for each of the spectroradiometers with the other fore optics was of the same order, although with lower degrees of freedom.

There are also uncertainties related to the kriging spatial interpolation method used, and these influence the position of the responsivity contours and the values predicted between the measurement points. A statistical prediction map was generated for each of the wavelengths assessed for both the ASD FieldSpec Pro and the GER 3700, each with 10° fore optic, and the maximum root mean squared errors (RMSE) were 0.048 and 0.027, respectively. The differences between the RMSE calculated for the ASD and that for the GER instrument are due to the difference in spatial sampling resolution selected (5 mm and 10 mm, respectively) and rather than any specific instrument phenomena. However, even given these uncertainties, the assessment of the extent of the area of measurement support and DRF of each spectroradiometer/fore optic combination presented here provides sufficient information on the probable shape, size, and level of responsivity at spatial locations across the target area from which the spectroradiometer receives radiance to enable field spectroscopy sampling strategies to be greatly improved.

IV. Conclusion

To enable a spectrum, or parts of a spectrum, recorded by a field spectroradiometer to be related to physical properties, or to classifications of type, of target surfaces of interest, it is necessary to know the spatial extent of the surface from which radiance is received, that is the area of measurement support. The responsivity of the spectroradiometer to radiance from within that area, i.e., the "weighting" given to radiance from any point within the area, is assumed to be equal. However, the FOV, normally specified by spectroradiometer manufacturers, does not provide the necessary information. At best, a FOV only describes one of the two parameters necessary to calculate spatial extent. These are the diameter of a circular area from which radiance may be received by a spectroradiometer and the distance from the apex of a triangle to the target surface which can only be approximated as the focal point of the fore optic is unknown. In addition, the FOV gives no indication of instrument responsivity to radiance from different locations within the area from which that radiance is received. More specifically, the use of the term FOV is misleading as it leads field spectroscopists to assume that: 1) the area of measurement support is circular (although in their manuals GER do advise against this assumption); 2) that there is an "edge" to this area that can be clearly defined, although a level of responsivity is never stated; and 3) that radiance received from any point within the area of measurement support is equally "weighted" within the integrated spectrum recorded.

This research has shown that when the 10° lens-based fore optic is used, the ASD system does not have a FOV, but that each fiber within the fiber optic bundle receives radiance from different areas within the area of measurement support and transmits this radiance to the sole spectrometer to which that fiber is attached. Each fiber has in effect its own FOV, leading to each of the three spectrometers integrating radiance from different areas (and these areas appear only to overlap toward the extremities of each fiber/spectrometer's responsivity) into the spectral range recorded by that spectrometer. It should also be noted that as the distribution of fibers to the spectrometers are randomized at the time of manufacture, each ASD FieldSpec Pro system will have a unique DRF, and hence the shape and coverage of the potential area of measurement support will be unique to each instrument. The area of measurement support has also been shown to extend well beyond that that the FOV parameter would define, yet, at the 5% responsivity level, there remain areas within the nominal FOV from which little or no radiance is received either by each or by all of the spectrometers. When the 5° lens-based fore optic was used, although each fiber still receives, and hence each spectrometer measures, radiance from distinctly different areas, the areas of overlap are greater, and the areas from which radiance is received by only one spectrometer are significantly less than found with the 10° fore optic, when the 5% responsivity level is considered. In addition, the extent of the area from which radiance is received much more closely approximates to that which the nominal FOV would suggest and does so at both the 5% or 50% responsivity levels, indicating a significant improvement in characteristics over the 10° fore optic (although the term FOV still has little relevance) at a 1-m sampling distance. It should be noted, however, that the when the 18° fore optic which has no lens is used, the term FOV is less misleading as the specified FOV included angle is being defined by either the field stop or the numerical aperture of the fibers or both. Each fiber still has its own FOV, but as all these FOVs effectively overlap each other, each spectrometer is measuring radiance from all areas within the area of measurement support, similar to the manner described by [38] for the fiber bundle without a fore optic. In addition, the area of measurement support and DRF measured in this research for the 18° fore optic are a reasonable approximation of that assumed by field spectroscopists. It just remains for the manufacturer to state a responsivity limit and the DRF to be defined to more fully specify the spectroradiometer/18° fore optic combination. It should also be noted however that for the FieldSpec Pro model used here, there was no method of determining if any fibers in the bundle were not transmitting radiance to their respective spectrometer without making DRF measurements or returning the instrument to the manufacturer for assessment. However, ASD have now incorporated a reverse illumination mechanism within their latest full wavelength spectroradiometer to allow the fibers to be checked.

For the GER 3700 system with the 10° lens-based fore optic, the area of measurement support more closely approximates a square or a rectangle, as the manufacturer suggests, than to a circle. The areas of measurement support for the VNIR and SWIR spectrometers with this fore optic do display different shapes, with those of the SWIR spectrometers more rectangular than square. There is also a spatial and spectral shift in the responsivity of the VNIR spectrometer, with more "weighting" given to blue wavelengths of light from the right and infrared wavelengths from the left of the target surface, while along the axis in alignment with the instruments entrance slit, no spectral shift is evident. When the 3° fore optic is fitted, the area of measurement support of each spectrometer appeared to be square and aligned, there was little evidence of an infrared spectral shift, and the blue shift was less pronounced, indicating, as for the ASD with 5° fore optic, an improvement over the wider angles lens-based fore optic. Again, as was observed for the ASD system, when the fiber optic accessory was used with the GER 3700, there was a significant improvement in the DRF. The DRF was found to be approximately Gaussian, concentric, and overlapping for each of the spectrometers.

For heterogeneous earth surface targets, the use of diagnostic spectral absorption and reflectance features, or indices derived from these, as proxies for state variables, or the use of spectra from such targets having classifications assigned in proportion of specific elements within the target area, is dependent on the reflected radiance being recorded being from a known and quantifiable target area. With heterogeneous target surfaces, and most natural earth surfaces, targets are heterogeneous to some degree, if the DRF is not uniform, if spatial coverage is incomplete and if the shape and area of measurement support are different from that assumed, then the components considered to be within the scene may not be quantified or correct proportions assumed. Hence, the properties of the assumed target area will be inaccurately represented in the actual radiance recorded or reflectance calculated. The contribution of individual scene components to gross radiance recorded may be excluded or over emphasized leading to erroneous classification of the surface or inaccurate quantification of physical and chemical variables derived from spectral indices.

It should be noted that the DRFs reported here are for specific instrument/fore optic combinations at the specified measurement distances, sampling resolutions, and for the lamp filament size used, and different results may be found if other instrument/fore optic and measurement configurations are used as; the ASD instrument fiber distribution will vary, as may the SVC instrument optical path; fore optic design and materials will effect the light passing through them; measurement distances may lead to the area of measurement support being in or out of focus; and the sampling resolution will effect phenomena recorded as will the lamp filament size. However, the results reported here have significant implications for the measurement of surface radiance. The wavelength-dependent spatial variability of the DRF and irregularly defined areas of measurement support evident from this study indicate that the assumption that the systems have uniform and regularly defined FOVs is invalid. Having knowledge of an instrument's DRF, and hence being able to define the area of measurement support and responsivity, of a field spectroradiometer is necessary but not alone sufficient to improve field spectroscopy measurements. It is also necessary to consider the heterogeneity of the target surface and statistically assess the quantity of

individual measurements required to acquire a representative mean of the radiance spectrum of the target of interest. A practical solution which quantifies the uncertainty of radiance from heterogeneous targets resulting from a nonuniform DRF may be to include multiple measurements of radiance spectra measured from nadir while rotating the instrument fore optic about its optical axis and to indicate a standard error per wavelength for the mean spectrum determined. A modeling study investigating effects that the DRFs of the instrument/fore optic systems reported here would have on reflectances recorded from heterogeneous earth surfaces, and on biochemical indices derived from these reflectance spectra, has now been conducted and will be reported at a later date and recommendations to improve field sampling strategies will be suggested.

The research reported here suggests that the use of a field stop aperture in place of a lens or the optimization of lens and, possibly, optical path design could give a more uniform DRF. However, repositioning lenses with respect to the instrument entrance slits will cause some defocusing of the image, improving the uniformity of directional response but with a possible reduction in system responsivity. Other options for improving the uniformity of the ASD lens fore optics could possibly be in the use of optical mixers or holographic diffusers positioned between the fiber optic bundle and the lens, although, again, these options may cause some reductions in systems responsivity. Indeed, after being advised of the work reported here, ASD now on request incorporate an optical mixer (a "scrambler") into the ASD pistol grip. It should also be noted that the latest ASD full wavelength system, the FieldSpec 3, does incorporate a method by which the operator can check the integrity of the fibers in the optical bundle without access to a spectroscopy darkroom or returning the instrument to the manufacturer. SVC have also considered the results reported here and optimized the alignment of elements in the optical path of their new instrument, the HR-1024, and make a more symmetric 8° fore optic and a bare fiber option available. Initial indications are that the DRFs of these systems and accessories greatly improve the DRFs of each system. These improved spectroradiometric systems will now be assessed and improvement in DRF and consequential changes in system sensitivity will also be reported at a later date.

ACKNOWLEDGMENT

This research was undertaken as part of the research and development program of the NERC FCF. Acknowledgement and thanks are given to the staff at ASD and SVC who assisted this research team gain a fuller understanding of their instruments and who both constructively considered the suggestions for improvement made in this paper. The authors also wish to thank the anonymous reviewers for their constructive comments, which improved the presentation of this work.

REFERENCES

[1] E. J. Milton, "Principles of field spectroscopy," *Int. J. Remote Sens.*, vol. 8, pp. 1807–1827, Dec. 1987.

[2] M. D. King, J. L. France, F. N. Fisher, and H. J. Beine, "Measurement and modelling of UV radiation penetration and photolysis rates of nitrate and hydrogen peroxide in Antarctic sea ice: An estimate of the production rate of hydroxyl radicals in first-year sea ice," *J. Photochem. Photobiol. A, Chem.*, vol. 176, no. 1–3, pp. 39–49, 2005.

[3] A. Chappell, T. M. Zobeck, and G. Brunner, "Using bi-directional soil spectral reflectance to model soil surface changes induced by rainfall and wind-tunnel abrasion," *Remote Sens. Environ.*, vol. 102, no. 3/4, pp. 328–343, 2006.

[4] G. Ferrier, B. T. Rumsbya, and R. J. Pope, "Application of hyperspectral remote sensing data in the monitoring of the environmental impact of hazardous waste derived from abandoned mine sites," *J. Geol. Soc. Lond., Special Publ.*, vol. 283, pp. 107–116, Jan. 2007.

[5] K. Anderson and N. Kuhn, "Variations in soil structure and reflectance during a controlled crusting experiment," *Int. J. Remote Sens.*, vol. 29, no. 12, pp. 3457–3475, Jun. 2008.

[6] G. Ferrier, K. Hudson-Edwards, and R. Pope, "Characterisation of the environmental impact of the Rodalquilar mine, Spain by ground-based reflectance spectroscopy," *J. Geochem. Exploration*, vol. 100, no. 1, pp. 11–19, Jan. 2009.

[7] H. Croft, K. Andersona, and N. Kuhn, "Characterizing soil surface roughness using a combined structural and spectral approach," *Eur. J. Soil Sci.*, vol. 60, no. 3, pp. 431–442, Jun. 2009.

[8] S. L. Ustin, A. A. Gitelsona, S. Jacquemoud, M. Schaepman, P. Gregory, G. P. Asner, J. A. Gamon, and P. P. Zarco-Tejada, "Retrieval of foliar information about plant pigment systems from high resolution spectroscopy," *Remote Sens. Environ.*, vol. 113, no. Suppl. 1, pp. S67–S77, Sep. 2009.

[9] M. Smith, T. Stevens, A. A. Mac Arthur, T. Malthus, and H. Lu, "Characterising Chinese loess stratigraphy and past monsoon variation using field spectroscopy," *Quaternary Int.*, vol. 234, no. 1/2, pp. 145–158, Apr. 2011.

[10] F. Visser and N. Smolar-Zvanut, "Detecting submerged macrophytes in a UK chalk stream using field spectroscopy," in *Proc. Annu. Conf. Remote Sens. Photogramm. Soc.*, 2009, pp. 541–547.

[11] S. Hamylton, "Estimating the coverage of coral reef benthic communities from airborne hyperspectral remote sensing data: Derivatives, multiple discriminant function analysis and linear spectral unmixing," *Int. J. Remote Sens.*, vol. 32, no. 24, pp. 9673–9690, Dec. 2011.

[12] T. Schmid, M. Koch, and J. Gumuzzio, "Multi-sensor approach to determine changes of wetland characteristics in semi-arid environments (Central Spain)," *IEEE Trans. Geosci. Remote Sens.*, vol. 43, no. 11, pp. 2516–2525, Nov. 2005.

[13] S. J. Lavender, M. Pinkerton, G. Moore, J. Aiken, and D. Blondeau-Patissier, "Modification to the atmospheric correction of SeaWiFS ocean colour images over turbid waters," *Cont. Shelf Res.*, vol. 25, no. 4, pp. 539–555, Mar. 2005.

[14] K. Anderson, E. J. Milton, and E. M. Rollin, "Calibration of dual-beam spectroradiometric data," *Int. J. Remote Sens.*, vol. 27, no. 5, pp. 975–986, Mar. 2006.

[15] D. S. Boyda, J. A. Entwistle, A. G. Flowers, R. P. Armitage, and P. C. Goldsmith, "Remote sensing the radionuclide contaminated belarusian landscape: A potential for imaging spectrometry?," *Int. J. Remote Sens.*, vol. 27, no. 10, pp. 1865–1874, May 2006.

[16] J. M. Huckle, R. H. Marrs, and J. A. Potter, "Characterising the salt-marsh resource using multi-spectral remote sensing: A case study of the Dee estuary in north-west England," *J. Pract. Ecol. Cons*, vol. 6, pp. 1–22, 2006.

[17] C. E. Hasselwimmera, T. R. Riley, and J. G. Liu, "Assessing the potential of multispectral remote sensing for lithological mapping on the Antarctic Peninsula: Case study from eastern Adelaide Island, Graham Land," *Antarctic Sci.*, vol. 22, no. 3, pp. 299–318, 2010.

[18] E. M. Rollin, E. J. Milton, and K. Anderson, "The role of field spectroscopy in airborne sensor calibration: The example of the NERC CASI," in *Proc. Conf. Field Spectral Meas. Remote Sens.*, Southampton, U.K., Apr. 15–16, 2002.

[19] R. J. Aspinall, W. A. Marcus, and J. W. Boardman, "Considerations in collecting, processing, and analysing high spectral resolution hyperspectral data for environmental investigations," *J. Geophys. Syst.*, vol. 4, no. 1, pp. 15–29, 2002.

[20] E. Karpouzli and T. Malthus, "The empirical line method for the atmospheric correction of IKONOS imagery," *Int. J. Remote Sens.*, vol. 24, no. 5, pp. 1143–1150, 2003.

[21] B. C. Hadley, M. Garcia-Quijano, J. R. Jensen, and J. A. Tullis, "Empirical versus model-based atmospheric correction of digital airborne imaging spectrometer hyperspectral data," *Geocarto Int.*, vol. 20, no. 4, pp. 21–28, Dec. 2005.

[22] E. J. Milton, M. Schaepman, K. Anderson, M. Kneubühler, and N. Fox, "Progress in field spectroscopy," *Remote Sens. Environ.*, vol. 113, no. Suppl. 1, pp. S92–S109, Sep. 2009.

[23] L. Kumar, K. Schmidt, S. Dury, and A. Skidmore, "Imaging spectrometry and vegetation science," in *Remote Sensing and Digital Image Processing*,

vol. 4, F. van der Merr and S. M. de Jong, Eds. London, U.K.: Kluwer, 2001.
[24] P. M. Mather, *Computer Processing of Remotely-Sensed Images*, 3rd ed. Chichester, U.K.: Wiley, 2004.
[25] P. M. Atkinson and P. Aplin, "Spatial variation in land cover and choice of spatial resolution for remote sensing," *Int. J. Remote Sens.*, vol. 25, no. 18, pp. 3687–3702, Sep. 2004.
[26] B. Robinson, *Electro-Optical Non-Imaging Sensors*, vol. 1, R. N. Colwell, Ed. Bethesda, MD: Amer. Soc. Photogramm., 1983.
[27] M. Schaepman, "Calibration of a field spectroradiometer: Calibration and characterization of a non-imaging field spectroradiometer supporting imaging spectrometer validation and hyperspectral sensor modelling," Ph.D. dissertation, Remote Sens. Lab., Univ. Zurich, Zurich, Switzerland, 1998.
[28] *ASD FieldSpec Pro: User's Guide, Revision C*, ASD, Boulder, CO, Jan., 2002.
[29] *GER 3700 Spectroradiometer User Manual*, 2nd ed., SVC, Poughkeepsie, New York.
[30] *Technical Guide*, 4th ed., ASD, Boulder, CO, 1999.
[31] T. H. Painter, "Correspondence," *J. Glaciol.*, vol. 57, no. 201, pp. 183–185, 2011.
[32] "Methods of characterizing illuminance meters and luminance meters," Comm. Int. L'Eclairage, Vienna, Austria, Tech. Rep. 69, 1987.
[33] K. Anderson, "Temporal variability in calibration target reflectance: Methods, models and applications," Ph.D. dissertation, Univ. Southampton, Southampton, U.K., 2005.
[34] E. Milton and E. M. Rollin, "Estimating the irradiance spectrum from measurements in a limited number of spectral bands," *Remote Sens. Environ.*, vol. 100, no. 3, pp. 348–355, 2006.
[35] N. P. Fox, "Traceability to SI for EO measurements," *CEOS WGCV Cal/Val Newslett.*, vol. 9, pp. 1–9, 2001.
[36] K. Johnston, J. M. Ver Hoef, K. Krivoruchko, and N. Lucas, *Using ArcGIS Geostatistical Analyst: GIS by ESRI*. Redlands, CA: ESRI, 2001.
[37] E. H. Isaaks and R. M. Srivastava, *An Introduction to Applied Geostatistics*. Oxford, U.K.: Oxford Univ. Press, 1989.
[38] *FieldSpec 3 User Manual, Revision C*, ASD, Boulder, CO, 2005.

Alasdair Mac Arthur received P.G Dip. in GIS and Remote Sensing from Manchester Metropolitan University, Manchester, U.K., in 2002, the M.Sc. degree in environmental decision making from the Open University, Barcelona, Spain, in 2004, and the Ph.D. degree in field spectroscopy and radiative transfer modelling from the University of Edinburgh, Edinburgh, U.K. in 2012.

He previously worked in conservation management and planning of protected areas in Scotland. He is currently the Operations Manager with the Natural Environment Research Council, Field Spectroscopy Facility, School of Geosciences, University of Edinburgh, U.K. He conducts research and advises on field spectroscopy methodologies and the performance and characteristics of spectroradiometers and optical sensors for environmental remote sensing and has research interests in the optical remote sensing of *Calluna vulgaris*-dominated peatlands.

He is a Fellow of the Royal Geographical Society.

Christopher J. MacLellan received the B.Sc. degree in physics from the University of Edinburgh, Edinburgh, U.K., in 1981.

He has worked in industry where he specialized in the design, manufacture, and calibration of light measurement instrumentation with Macam Photometrics Ltd, Livingston, U.K., and Optronic Laboratories Inc., Orlando, FL. He is currently the Equipment Manager with the Natural Environment Research Council, Field Spectroscopy Facility, School of Geosciences, University of Edinburgh, where his responsibilities include equipment test and calibration, system performance measurements, and new sensor design.

Tim Malthus received the Ph.D. degree in limnology from the University of Otago, Otago, Netherlands, in 1986. Through postdoctoral positions at the Centre for Limnology, Netherlands (1986–1988) and at the University of Nottingham, Nottingham, U.K., in (1988–1991).

He worked on remote sensing related research in inland water quality and in vegetation science. He then moved on to tenured posts at the University of Wolverhampton (1991–1994) and University of Edinburgh, Edinburgh, U.K., in (1994–2009). At Edinburgh, he became Director of the NERC Field Spectroscopy Facility in 2004, a position he held until taking up his current post as Research Program Leader in Environmental earth Observation in CSIRO's Division of Land and Water, Canberra, Australia. His research interests primarily focus on calibration and validation, field spectroscopy, and inland water quality.